**David E. Gilsinn**
Mem. ASME
Mathematical and Computational Sciences Division,
National Institute of Standards and Technology,
Gaithersburg, MD 20899-8910
e-mail: dgilsinn@nist.gov

**Alice V. Ling**
Air Force Research Laboratory
Kirtland AFB, NM 87117

# Comparative Statistical Analysis of Test Parts Manufactured in Production Environments

*Estimating error uncertainties arising in production parts is not a well-understood process. An approach to estimate these uncertainties was developed in this study. Machine tool error components were measured on a three-axis vertical machining center. Multiple parts were produced on the measured machining center then measured on a coordinate measuring machine. Uncertainty models for hole-center to hole-center lengths and orthogonalities were developed using measured machine tool errors. These estimated uncertainties were compared against measured uncertainties. The main conclusion from the study is that the Law of Propagation of Uncertainties can be used to estimate machining uncertainties.* [DOI: 10.1115/1.1645876]

## 1 Introduction

Given a particular machine tool, estimating beforehand the errors in features for the parts produced by that machine is not a clearly defined process. Although there are general guides for reporting uncertainties in experiments (see ISO [1], Taylor and Kuyatt [2], American National Standards Institute [3]) to the authors' knowledge there have been no published practical case studies on how to estimate uncertainties of errors of machined part features in production environments. This paper describes a case study in which a part was specified and given to a production machine shop with an order to make twenty-one copies of the part on the same machine. The part designed had drilled and milled holes and a circular slot (see Fig. 1). The shop manager independently selected a three-axis machining center on the shop floor for the production job. With shop assistance the error components of the machine tool were measured multiple times using a laser ball bar (LBB) but due to shop rules the machine metrology and parts manufacturing could only be accomplished in business day increments with a maximum of five business days allowed for the entire project. An error model of the machining center was developed and axis error uncertainties estimated by using the propagation of error formula from the ISO Guide [1]. An analytic formula was developed and then used to estimate the variation in distance between selected features, such as hole centers. To estimate uncertainties of orthogonality of peripheral hole centers, it was determined that a Monte Carlo technique worked best, where a detailed explanation is found in Section 3.5. All twenty-one parts were measured on a coordinate measuring machine (CMM) and an analysis of variance technique was used to separate the uncertainties generated by the measurement and by manufacturing. Two types of features were analyzed in this study: (1) uncertainties of the distance between hole centers and (2) orthogonalities of peripheral hole centers. The essential techniques employed are presented in this paper in order to form a basis for estimating the uncertainties associated with production parts. For a more detailed discussion, along with supporting metrology data, see Gilsinn and Ling [4].

Various authors have discussed different aspects of the problem of machining uncertainties. Under a controlled set of experiments, Wilhelm, Srinivasan and Farabaugh [5] have demonstrated that the measured behavior of the machine tool could be related to variations found in prismatic part features cut on that machine tool. The machining and metrology conditions were tightly controlled. A horizontal machining center was used. Parts were produced with features similar to those in this study. The results indicated that most part errors fell within two standard deviations of measured machine errors. However, under uncontrolled conditions, a recent study by Chatterjee [6] has shown that there is a significant deviation in machine tool performance between static and operating conditions, where machine parameters are likely to vary due to cutting and thermal loads. Shin and Wei [7] developed a kinematic model for a multi-axis machine tool in order to predict deterministic errors. They added stochastic terms to the predicted errors and theoretically estimated the means and variances of the kinematic errors, but provided no experimental data comparison.

The inaccuracies of drilling operations have been studied by a number of authors. These results, however, are in general not formulated in terms of uncertainties. Kaminski and Crafoord [8] state that drilling operations give rise to forces in the $X$, $Y$ and $Z$ directions as well as torque. They found that the tool deflects more under dynamic cutting conditions than under static simulated force loads. Lehtihet and Gunasena [9] use a simulation to show the influence of tolerance specification, size of the tolerance zone, hole size density, and production errors on the probability of producing an acceptable hole. Lee, Eman and Wu [10] discuss a mathematical model for drill wandering motion to explain the formation of odd-sided polygonal holes during initial penetration. Fujii, Marui and Ema [11–13] find that the drill point deflects along an elliptical orbit during whirling vibration. Magrab and Gilsinn [14] model a drill bit as a twisted Euler beam under axial loading that is clamped at both ends. The representative set of modes obtained exhibit a complex out-of-plane twisting-type motion that suggests a possible explanation for the out-of-roundness of certain drilled holes.

In a work that relates to the current study Shen and Duffie [15–16] developed an uncertainty analysis method that allows the modeling and computation of component error uncertainty sources that lead to coordinate transformation uncertainties. They show how uncertainties propagate in the homogeneous transformations of points, products of transformations and inverse transformations. They characterize the uncertainties associated with workpiece positions and orientations in terms of two components, a bias and a precision uncertainty component. They demonstrate that the bias and precision components can be propagated independently and combined to represent the uncertainties of the coordinate transformation relations. They validate the method by using Monte Carlo simulation (Bauer [17]) but do not report experimental data.

Several recent papers relate measurement uncertainties in

Contributed by the Manufacturing Engineering Division for publication in the JOURNAL OF MANUFACTURING SCIENCE AND ENGINEERING. Manuscript received Oct 2003. Associate Editor: E. C. DeMeter.


**Copyright © 2004 by ASME**

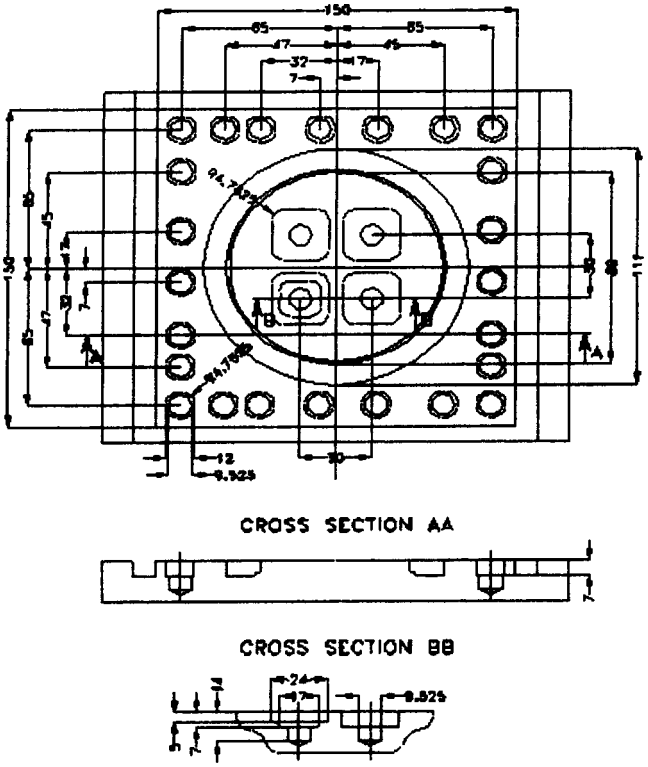


**Fig. 1 Test part specifications. Dimensions are in millimeters.**

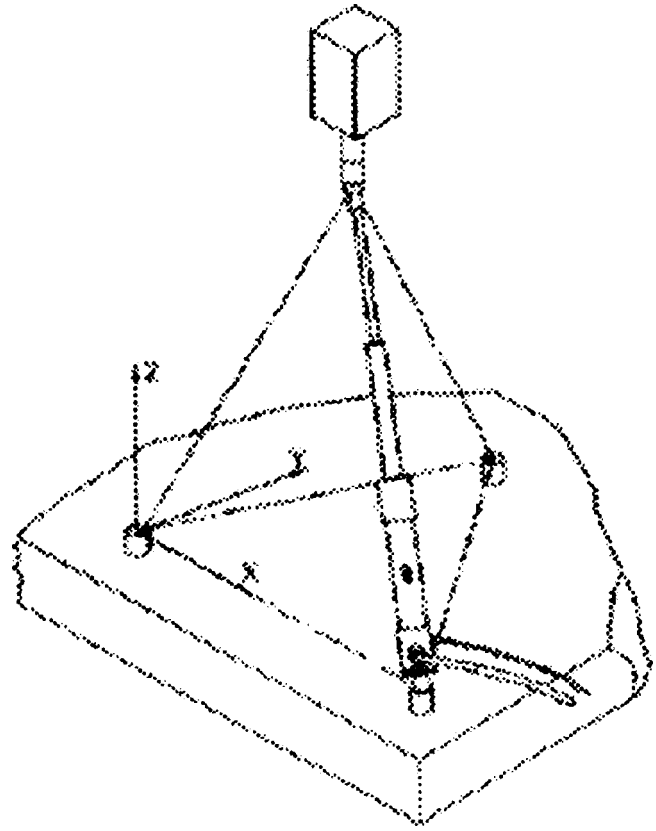

**Fig. 2 Laser Ball Bar (LBB) configuration**

CMM measurements to the sampling strategy. Yau [18] proposed a general mathematical basis for representing vectorial tolerances. He developed a nonlinear, best-fit algorithm to evaluate vector tolerances for both analytic geometric elements and free-form surfaces. He then studied the uncertainty of the best-fit result caused by the sampling strategy and dimensional errors. Phillips, Borchardt, Estler and Buttress [19] examine the uncertainty of small circular features as a function of sampling strategy, i.e. the number and distribution of measurement points. They study the effect of measuring a circular feature using a three-point sampling strategy and show that the measurement uncertainty varies by four orders of magnitude as a function of the angular distribution of the measurement points.

This paper is organized as follows. Section 2 briefly describes the machine tool measurement procedure and the part design. Section 3 describes a kinematic model of a three-axis machine tool along with the methods of estimating errors for point location, linear distances, and orthogonalities. The uncertainty estimates for CMM measurements of the parts are given in Section 4. Some observations about the case study are given in Section 5, with some final conclusions given in Section 6.

## 2 Machine Metrology and Part Design

The milling machine used to manufacture the test parts was a three-axis vertical machining center with an *X*-axis (Longitudinal table) travel of 1020 mm (40 in), a *Y*-axis (Cross table) travel of 762 mm (30 in), and a *Z*-axis (Vertical head) maximum travel of 560 mm (22 in). The programming resolution for all three axes was 0.001 mm (0.0001 in). The repeatability was reported by the machine manufacturer as 0.005 mm (0.0002 in) by the VDI 3441 method and $\pm 0.0025$ mm ($\pm 0.0001$ in) by the JIS 6330 method.

The part, shown in Fig. 1, was designed to illustrate several characteristics of the machining center. The holes around the outer edge have several purposes. First, drilled holes in the center were used to compute uncertainties in drilled hole-center positioning. The "squared" outer holes allowed comparison of milled hole-centers to the drilled hole-centers. The large square with 150 mm sides was machined to check the orthogonality or perpendicularity of the machine's *X* and *Y*-axes. This property is sometimes called squareness. The large internal circular features will not be discussed in this paper.

Although ASME B5.54 [20] outlines techniques for performing parametric error measurements of machine tools using instruments such as laser interferometers, precision straight edges, capacitance gauges, and electronic levels, a laser ball bar (LBB) was used to make measurements of the spatial position of the tool using a technique called trilateration (see Fig. 2). Trilateration is a technique in which a tetrahedron is formed with three base points (vertices) attached to the machine table, and the fourth attached to the tool holder. The three base points define a coordinate system. Simple geometric relationships allow the spatial coordinates of the fourth point or tool to be determined relative to this coordinate system. If the base sockets are aligned parallel to one machine axis and the plane formed by the base is coplanar with the table surface then the measurement of errors with respect to the *X*-axis and *Y*-axis motions are taken at the table surface level. As the tool moves through space relative to the table, the lengths of the edges change causing the tetrahedron to deform. The LBB uses an interferometric technique to measure the lengths of the tetrahedron edges and thus the tool position. The resulting measurement includes all effects that can cause positioning error: geometric, thermal and elastic. Various error components of the machine tool are measurable by the LBB including linear displacement errors, straightness errors, squareness errors as well as roll, pitch and yaw errors. For a detailed discussion of the LBB and a comparison of the results of LBB measurements with ASME B5.54 measurements see Ziegert and Mize [21]. The spatial measurement accuracy of the LBB was tested on the MOORE M60 CMM at the Y12 facility, at Oak-Ridge, Tennessee, where it was found that the mean difference between the LBB measured coordinates and the

M60 reported coordinates for all measured points was 0.65 $\mu$m, with a standard deviation of 0.1 $\mu$m (see Srinivasa and Ziegert [22]). For a discussion of the use of a LBB in dynamic path measurements see Schmitz and Ziegert [23] and in modeling and predicting thermally induced errors see Srinivasa and Ziegert [22].

The machine measurements were made by the following procedure. Five passes in both a forward and reverse direction were made consecutively in a large work volume that contained the smaller work volume that enclosed the machined parts. The number of passes made was limited by machine time available, which was an eight-hour business day. This provided ten sets of data as a basis to model each of the error components of the machining center. The LBB measured all twenty-one-error components that characterize the errors for a three-axis machining center. The data was used to develop regression models of the error components as functions of the positions along each machine axis.

## 3 Part Uncertainty Through Model Prediction

Predicting part uncertainty by using a kinematic machine tool model required a number of approximations. First, various error components were assumed to only enter in a linear fashion. Second, analysis of the measured machine error components indicated thermal drift between measurement repetitions. Since thermal drift could not be controlled during the measurement process, the measured curves were treated as bona fide repeat curves. The resulting uncertainty models were therefore assumed to be conservative. Finally, in order to estimate the orthogonality of peripheral hole center alignment, Monte Carlo simulation was used. This was done since the models predicted hole center errors in both of the $X$ and $Y$ components, and a standard least squares linear fit could not be directly applied because it would require that there be errors in only one of the components.

**3.1 Kinematic Model for a Machining Center.** The construction of the kinematic model followed the procedure of Donmez [24]. The axis system assumed has the $X$-axis directed towards the right, the $Y$-axis toward the machine, and the $Z$-axis directed vertically. Since uncertainties were estimated based on planar locations of such points as hole centers in Fig. 1, only the planar portion of the kinematic model is given here. The following error components enter into the planar kinematic error model for the three axis mill: $E_1=\delta_x(x)$, $X$-axis scale error; $E_2=\delta_y(x)$, $Y$-straightness of $X$; $E_3=\delta_y(y)$, $Y$-axis scale error; $E_4=\delta_x(y)$, $X$-straightness of $Y$; $E_5=\varepsilon_x(x)$, $X$-rotation of $X$ (roll of $X$); $E_6=\varepsilon_y(x)$, $Y$-rotation of $X$ (pitch of $X$); $E_7=\varepsilon_z(x)$, $Z$-rotation of $X$ (yaw of $X$); $E_8=\varepsilon_x(y)$, $X$-rotation of $Y$ (pitch of $Y$); $E_9=\varepsilon_y(y)$, $Y$-rotation of $Y$ (roll of $Y$); $E_{10}=\varepsilon_z(y)$, $Z$-rotation of $Y$ (yaw of $Y$); $E_{11}=\alpha_{xy}$, angle between the $X$ and $Y$-axes with $Y$ motion. A generalized straightness error due to $X$-straightness error of $Y$-motion is given by $E_4-E_{11}\Delta y$, where $\Delta y$ represents incremental steps along the $Y$-axis. The final planar error equations used to analyze the data are given by the following equations.

$$E_x=E_1+E_4+zE_6+yE_7+zE_9+yE_{10}-yE_{11}$$
$$E_y=E_2+E_3-zE_5-xE_7-zE_8 \tag{1}$$

For the selected machine tool an effective $Z$ value for the production of the parts was estimated as follows. Shop personnel indicated that although the maximum travel for the $Z$-axis was 560 mm (22 in) the useful travel of the $Z$-axis without tool or chuck was 431.8 mm (17 in.). The length of the tool used, plus chuck insert, was 304.8 mm (12 in.). This produced an effective $Z$-travel of 127 mm (5 in.). Any local $Z$-axis travel to produce the required parts was considered small relative to the $X$ and $Y$-axis travel so that, in the model, $Z$ was taken as fixed at 127 mm.

**3.2 Regression Models for the Component Errors.** In order to compare the results obtained from modeling measured machine tool errors with calculated errors on the machined parts measured by a CMM, the first task was to mathematically align the coordinate systems of the machine tool and the CMM so that the origins and axes overlapped. Since the data taken by the LBB was measured relative to the machining center's coordinate axis, formulating models from the LBB data required linking the part origin from the CMM measurements to the machine tool coordinate system.

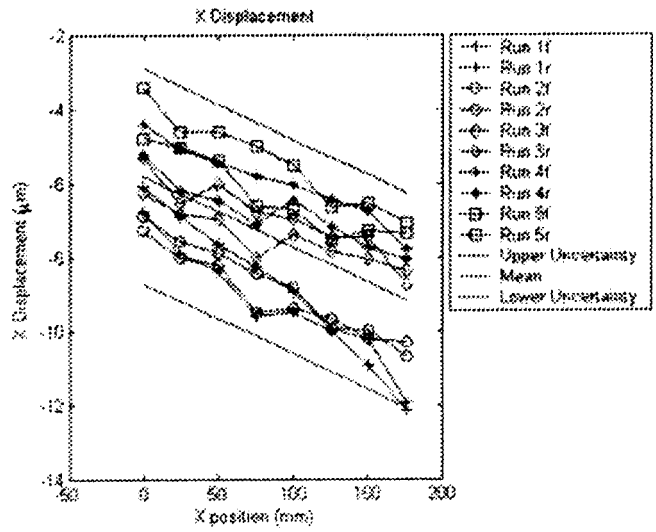


**Fig. 3 LBB measurements of machine tool error components showing the mean least squares trend line with uncertainty band using a coverage factor of two**

Figure 3 shows the shifted data values recorded by the LBB for the $X$-displacement component error, $E_1=\delta_x(x)$, along with uncertainty bands using a coverage factor of two (nominal 95% confidence). The other nine component errors show similar trends. The figure shows a linear trend over the work volume of the test parts. Linear regression models were fit to each of the nine data sets. Since eight of the measurement steps fell within the work volume of the part being milled, only the data from those eight entered the regression analysis. In that case eighty observations were made for each of ten error components. The measurements were normalized to part zero so that the zero point on the horizontal axis represented the part zero. The figure shows a definite effect of thermal conditions. There was a general tendency of the graphs for the displacement and straightness errors to rise as testing progressed. For this initial study, we aimed at minimizing the number of variations during the process. We desired to perform our study at a thermal equilibrium for the machine tool, which is the usual practice on a typical shop floor. However, the shop floor cooled down after normal working hours, which had a direct effect on the machine tool temperature and its geometrical error components. A future study might consider fully characterizing the thermal range of the machine and its direct correlation to errors on the production part. The angular error components rose through the third pass, with retreat indicating a reversal of rotation after about five hours of continual running. This thermal effect introduced a nonstationarity in the data such that traditional assumptions on the variance of sample repetitions would not apply, but for the purpose of this study we have elected to consider them as legitimate repeats and the resulting analysis is accepted as being conservative. The LBB measurement of the angular error, identified as the eleventh error, $E_{11}=\alpha_{xy}$, between the $X$ and $Y$ axes, was independent of coordinate position. Table 1 gives these angular errors measured by the LBB in arc seconds and radians. The mean error in radians, estimated standard deviation and degrees of freedom are also given. These were used to estimate a confidence interval for a future observation of the angular error. Table 2 gives the slope and intercepts for the linear trend equations describing the error components.

**Table 1 LBB measurements of the angular errors between the *X* and *Y* axes**

| Angular Error Between $X$ and $Y$ Axes | | |
|---|---|---|
| Pass # | Error (arcsec) | Error (radians) |
| 1 | −6.99 | −3.39−05 |
| 2 | −6.43 | −3.12$E$−05 |
| 3 | −7.39 | −3.58$E$−05 |
| 4 | −6.76 | −3.27$E$−05 |
| 5 | −6.79 | −3.29$E$−05 |
| | Mean | −3.33$E$−05 |
| | Est. Std. Dev. | 1.67$E$−06 |
| | Deg. Of Freedom | 4 |

**3.3 General Propagation of Uncertainties Using the Kinematic Model.** In order to estimate the uncertainties a simplifying assumption was made that the individual error terms were uncorrelated since it was difficult to estimate or measure the cross correlation terms for each component error. Since the LBB measurement instrumentation used did not allow simultaneous measurements of all component errors this assumption was necessary.

According to the *Law of Propagation of Uncertainty*, outlined in the ISO Guide [1], Taylor and Kuyatt [2], Coleman and Steele [25] and Wheeler and Ganji [26], if a variable $E$, such as those in Eq. (1), is a function of $N$ stochastic components that are uncorrelated.

$$E=f(E_1,\cdots,E_N) \tag{2}$$

The combined uncertainty of $E$, $\mathbf{u_c(E)}$, can be estimated in terms of the uncertainties of the components, ignoring second order terms, by

$$u_c^2(E)\approx\sum_{i=1}^{N}\left(\frac{\partial f}{\partial E_i}\right)^2 u^2(E_i) \tag{3}$$

The variances of the positioning errors in Eq. (1) can therefore be computed from the propagation of uncertainties law as

$$\begin{aligned} u_c^2(E_x)&=u^2(E_1)+u^2(E_4)+z^2u^2(E_6)+y^2u^2(E_7)+z^2u^2(E_9)\\ &\quad+y^2u^2(E_{10})+y^2u^2(E_{11})\\ u_c^2(E_y)&=u^2(E_2)+u^2(E_3)+z^2u^2(E_5)+x^2u^2(E_7)+z^2u^2(E_8) \end{aligned} \tag{4}$$

**Table 2 Error component coefficients**

| Kinematic Error Component Coefficients | | |
|---|---|---|
| | Displacement Slope Nondim. | Errors Intercept mm |
| $\delta_x(x)$ | −1.89$E$−05 | −5.83$E$−03 |
| $\delta_y(x)$ | −3.78$E$−06 | 4.17$E$−03 |
| $\delta_y(y)$ | −1.83$E$−05 | 4.35$E$−04 |
| $\delta_x(y)$ | −3.88$E$−06 | 3.40$E$−03 |
| | Rotational Slope Nondim. | Errors Intercept Radians |
| $\varepsilon_x(x)$ | 3.77$E$−09 | −3.44$E$−05 |
| $\varepsilon_y(x)$ | −3.06$E$−08 | −6.09$E$−06 |
| $\varepsilon_z(x)$ | −2.87$E$−08 | 3.06$E$−05 |
| $\varepsilon_y(y)$ | 3.77$E$−08 | 3.98$E$−05 |
| $\varepsilon_x(y)$ | −6.04$E$−09 | −6.57$E$−05 |
| $\varepsilon_z(y)$ | −5.62$E$−08 | 1.51$E$−05 |
| | $X$-$Y$ Axes Angle Slope Nondim. | Error Intercept Radians |
| $\alpha_{xy}$ | 0.00$E$+00 | −3.33$E$−05 |

To evaluate the uncertainties $u_c(E_x)$, $u_c(E_y)$, the uncertainties of individual error components were determined by using machine characterization data. These uncertainties were estimated from their equations. The methods are described in Montgomery and Peck [27]. Since the component errors are modeled as linear equations, their regression equations take the form

$$y=X\beta+r \tag{5}$$

where $r$ refers to the regression error and, in general, $y$ is an $n\times1$ vector of observations. $X$ is an $n\times2$ matrix of the regressor variables. $\beta$ is a $2\times1$ vector whose components are: $\beta_1$ the line intercept and $\beta_2$ the line slope. $r$ is an $n\times1$ vector of random errors. The least squares estimator of $\beta$ is given by the well-known formula

$$\hat{\beta}=(\mathbf{X^TX})^{-1}\mathbf{X^Ty}. \tag{6}$$

Given a coordinate, $x_1$, which could be along the $x$ or $y$ coordinate axis depending on the approximate error component equation that is being evaluated, the predicted value is computed as

$$\hat{\mathbf{y}}=\mathbf{x^T}\hat{\beta} \tag{7}$$

where $x^T=[1\ x_1]$ is the regressor variable. A point estimate of the future observation $y_0$ is given by (7) as

$$\hat{\mathbf{y}}_\mathbf{0}=\mathbf{x_0^T}\hat{\beta} \tag{8}$$

A confidence interval for this predicted observation is

$$\begin{aligned}\hat{\mathbf{y}}_\mathbf{0}-\mathbf{k_p}\sqrt{\hat{\sigma}^2(\mathbf{1}+\mathbf{x_0^T}(\mathbf{X^TX})^{-1}\mathbf{x_0})}\\ \leqslant\mathbf{y_0}\leqslant\hat{\mathbf{y}}_\mathbf{0}+\mathbf{k_p}\sqrt{\hat{\sigma}^2(\mathbf{1}+\mathbf{x_0^T}(\mathbf{X^TX})^{-1}\mathbf{x_0})}\end{aligned} \tag{9}$$

where $k_p$ is the coverage factor, taken here as $k_p=2$ [2]. This interval is referred to as a *prediction interval* for a future observation of $y_0$ [27]. It is more conservative than the confidence interval for the mean, but is more applicable for parts production since it depends both on the error of the fitted model and the error associated with future observations of parts. The term $\sqrt{\hat{\sigma}^2(\mathbf{1}+\mathbf{x_0^T}(\mathbf{X^TX})^{-1}\mathbf{x_0})}$ will be referred to as the *standard uncertainty* with the understanding that it is the standard error of a new observation given a value of the regressor variable. The expanded standard uncertainty is then

$$\mathbf{u}(\mathbf{x_0})=\mathbf{2}\sqrt{\hat{\sigma}^2(\mathbf{1}+\mathbf{x_0^T}(\mathbf{X^TX})^{-1}\mathbf{x_0})} \tag{10}$$

where

$$\hat{\sigma}^2=\frac{\mathbf{y^Ty}-\hat{\beta}^\mathbf{T}\mathbf{X^Ty}}{\mathbf{n-2}}. \tag{11}$$

Figure 3 shows the linear equation fit to the $X$-axis scale, $E_1$, data as well as the upper and lower uncertainty bands based on the interval in Eq. (9).

At this point we will show how the formulas above, used to estimate an uncertainty interval for the next observation for a linear regression problem, can also be used to estimate an uncertainty interval for the next sample of the angular error given in Table 1. Although the angular error model is considered to be a constant, the representation we select is given by Eq. (5) with the $y$ vector given by the five angular errors in Table 1 and the $X$ matrix given by $[\mathbf{1\,1\,1\,1\,1}]^\mathbf{T}$. The parameter estimates are then given by Eq. (6), which in this case is $\hat{\beta}=(X^TX)^{-1}X^TY=1/5\Sigma_{i=1}^5E_{11,i}=\overline{E}_{11}$. Thus the least squares model in this case is the mean of the samples. Furthermore, $x_0=[1]$, so that $\mathbf{x_0^T}(\mathbf{X^TX})^{-1}\mathbf{x_0}=\mathbf{1/5}$. The coverage factor is again selected as 2. In this case, the confidence interval for a future sample of the angular error between the $x$ and $y$ axes is given by

$$\overline{E}_{11}-2\sqrt{\frac{6}{5}\hat{\sigma}^2}\leqslant E_{11}\leqslant\overline{E}_{11}+2\sqrt{\frac{6}{5}\hat{\sigma}^2} \tag{12}$$

where

$$\hat{\sigma}^2=\frac{1}{4}\left(\sum_{i=1}^{5} E_{11,i}^2-\hat{\beta}\sum_{i=1}^{5} E_{11,i}\right) \tag{13}$$

which for the data in Table 1 is $2.88849e-12$ radian squared. Therefore the uncertainty interval for a future angular error observation, in radians, is

$$-3.70355e-5 \leqslant E_{11} \leqslant -2.95885e-5 \tag{14}$$

where the estimated standard deviation for a future sample is $1.86177e-6$ radians.

From the entries in Table 2 one can substitute estimates into the individual component error equations of the general form

$$y=\beta_2 x+\beta_1 . \tag{15}$$

The degree of freedom of each of the first ten estimates is seventy eight, since there are eighty samples used to estimate the linear error component functions, and the degree of freedom of the last is four. The estimates of $\sigma^2$ for each of the error components identified in Section 3.2 are given by

$$\begin{aligned}
\sigma_j^2&=\frac{1}{78}\left\{\sum_{i=1}^{80} (E_i-\beta_2 x_i-\beta_1)^2\right\}, \quad j=1,2,5,6,7\\
\sigma_j^2&=\frac{1}{78}\left\{\sum_{i=1}^{80} (E_i-\beta_2 y_i-\beta_1)^2\right\}, \quad j=3,4,8,9,10\\
\sigma_{11}^2&=\frac{1}{4}\left\{\sum_{i=1}^{5} (\alpha_{xy,i}-\beta_{72})^2\right\}.
\end{aligned} \tag{16}$$

With these one can now estimate the variances of the variables on the left of Eq. (15) at a specific point $(x_0,y_0)$ in the machine tool workspace. These are given by

$$\begin{aligned}
u^2(\hat{E}_j)&=\sigma_j^2\left\{\frac{1}{80}+\frac{(x_0-\overline{x})}{\Sigma_{i=1}^{80}(x_i-\overline{x})^2}\right\}, \quad j=1,2,5,6,7\\
u^2(\hat{E}_j)&=\sigma_j^2\left\{\frac{1}{80}+\frac{(y_0-\overline{y})}{\Sigma_{i=1}^{80}(y_i-\overline{y})^2}\right\}, \quad j=3,4,8,9,10\\
u^2(\hat{E}_{11})&=\sigma_{11}^2\left\{\frac{6}{5}\right\}.
\end{aligned} \tag{17}$$

In order to estimate a confidence interval of a future error response one must add the combined standard uncertainty about the mean at a point $(x_0,y_0)$ with the combined standard uncertainty about the mean $E$ and compute the square roots of

$$\begin{aligned}
u_{co}^2(\hat{E}_x)&=(u^2(\hat{E}_1)+\sigma_1^2)+(u^2(\hat{E}_4)+\sigma_4^2)+z_0^2(u^2(\hat{E}_6)+\sigma_6^2)\\
&\quad+y_0^2(u^2(\hat{E}_7)+\sigma_7^2)+z_0^2(u^2(\hat{E}_9)+\sigma_9^2)\\
&\quad+y_0^2(u^2(\hat{E}_{10})+\sigma_{10}^2)+y_0^2(u^2(\hat{E}_{11})+\sigma_{11}^2),\\
u_{co}^2(\hat{E}_y)&=(u^2(\hat{E}_2)+\sigma_2^2)+(u^2(\hat{E}_3)+\sigma_3^2)+z_0^2(u^2(\hat{E}_5)+\sigma_5^2)\\
&\quad+x_0^2(u^2(\hat{E}_7)+\sigma_7^2)+z_0^2(u^2(\hat{E}_8)+\sigma_8^2).
\end{aligned} \tag{18}$$

The prediction error at $(x_0,y_0)$ can be estimated by substituting Eq. (16) and Eq. (17) into Eq. (18) and use a coverage factor of two to write

$$\begin{aligned}
&E_x \pm 2\sqrt{u_{co}^2(\hat{E}_x)}\\
&E_y \pm 2\sqrt{u_{co}^2(\hat{E}_y)}
\end{aligned} \tag{19}$$

Equations (1), (18) and (19) were used to estimate the values in Table 3 for three points that were used as line end-points in the next section. The table shows the nominal $(x,y)$ location the $X$-axis and $Y$-axis error, the estimated error variance, uncertainty and expanded uncertainty.

**Table 3 Line end-point uncertainties**

| *X* Axis | | | | | |
|---|---|---|---|---|---|
| Hole Number | Nominal (mm) | Error ($\mu$m) | Variance ($\mu$m)$^2$ | Uncertainty ($\mu$m) | Expanded Uncertainty ($\mu$m) |
| 3 | 10 | 2.4 | 10.6 | 3.3 | 6.6 |
| 9 | 10 | 12.6 | 24.6 | 5.0 | 10.0 |
| 15 | 140 | 8.2 | 24.6 | 5.0 | 10.0 |
| *Y* Axis | | | | | |
| Hole Number | Nominal (mm) | Error ($\mu$m) | Variance ($\mu$m)$^2$ | Uncertainty ($\mu$m) | Expanded Uncertainty ($\mu$m) |
| 3 | 10 | 10.0 | 43.7 | 6.6 | 13.2 |
| 9 | 140 | 16.8 | 43.7 | 6.6 | 13.2 |
| 15 | 140 | 10.6 | 52.4 | 7.2 | 14.5 |

**3.4 Linear Distance Uncertainties.** Estimating distances between hole centers is a planar problem so we will only be concerned with the $x$ and $y$ errors at the hole centers. Suppose that two points, $(x_1,y_1)$ and $(x_2,y_2)$, are given on a part, such as the centers of two drilled holes. Each of these points has an error associated with it, given by $(E_x^1,E_y^1)$ and $(E_x^1,E_y^1)$. The estimated length, $L$, is then computed from

$$L^2=(x_1+E_x^1-x_2-E_x^2)^2+(y_1+E_y^1-y_2-E_y^2)^2 \tag{20}$$

and the nominal length, $L_0$, is computed from

$$\mathbf{L_0^2}=(\mathbf{x_1}-\mathbf{x_2})^2+(\mathbf{y_1}-\mathbf{y_2})^2. \tag{21}$$

Since the variance of the actual length is approximately the variance of the estimated length, i.e. $\mathbf{u_{co}^2(L_a)\approx u_{co}^2(L)}$, then, using Eqs. (20) and (21), the estimated variance of the actual length is given by

$$\begin{aligned}
u_{co}^2(L)&=\left[\frac{(x_1-x_2)}{L_0}\right]^2(u_{co}^2(E_x^1)+u_{co}^2(E_x^2))+\left[\frac{(y_1-y_2)}{L_0}\right]^2\\
&\quad\times(u_{co}^2(E_y^1)+u_{co}^2(E_y^2))
\end{aligned} \tag{22}$$

The validity of this equation depends on the statistical independence of the error terms on the right of Eq. (22).

Using Eq. (22) three length uncertainties were estimated. These were chosen to reflect the essential nature of the part uncertainties in general. The lengths chosen were the center-to-center lengths from hole number 3 to hole number 9, from hole 9 to hole 15, and finally from hole 3, to hole 15 as given in the part numbering scheme shown in Fig. 4. The estimates are given in Table 4. This table is consistent in that the uncertainties squared of the lengths between hole-centers are less than the sum of the squares of the component uncertainties.

**3.5 Hole Center Orthogonality Uncertainties.** If the part, shown in Fig. 1 and Fig. 4, were ideal, the line through holes 9 through 15 would lie at right angles to the lines through holes 9 through 3. However, real parts seldom, if ever, satisfy this property due to machine orthogonality errors. In general there is a small difference between the actual angle that the two lines form and a right angle. This is termed an orthogonality error. Due to inherent machine variability, the set of copies of the part was expected to have a distribution of orthogonality errors.

Since each of the hole-centers has a point uncertainty this means that there is error in both the $X$ and $Y$ positions of the center. This fact introduces a problem with finding the best line through the centers of the holes. Assume that we are given points $(\mathbf{x_1},\mathbf{y_1}),\cdots,(\mathbf{x_N},\mathbf{y_N})$ and we wish to find the least squares line through the points. The assumption behind the least squares estimation of coefficients is that the linear first order model can be written as $y=\beta_0+\beta_1 x+r$ where the $r$ term represents the devia-

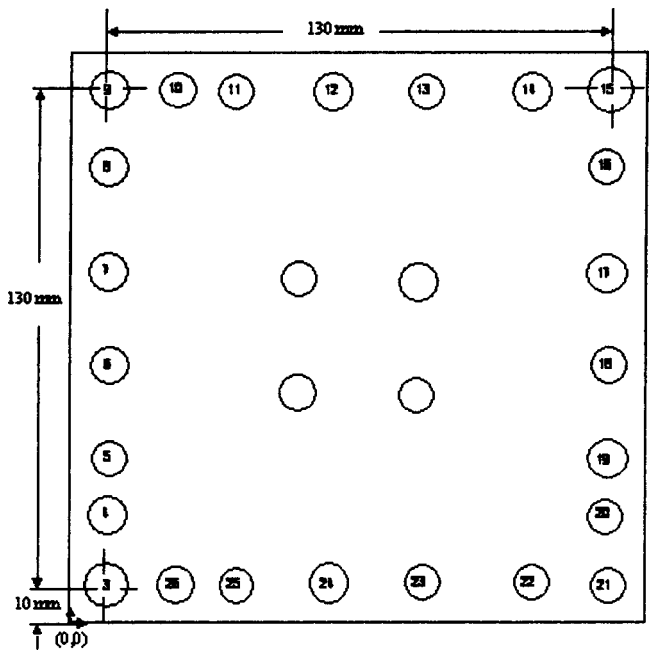


**Fig. 4 Numbered peripheral holes of Fig. 1**

tion in the $y$ variable from the line. Thus all of the error in the approximation is assumed to be relegated to the $y$ variable and the $x$ variable is assumed to have no error. For this application, we desire to fit equations to data in which both variables are subject to error. The relevant methods are called errors in variables (see Mandel [28]). Since the algorithms for this form of data fitting are not universally available we chose a Monte Carlo approach in which the $x$ and $y$ distributions of the hole centers were sampled a large number of times, horizontal and vertical lines fit to the resulting points, and angular differences from right angles computed. The uncertainty in this large sample of orthogonality errors could then be computed.

To generate an orthogonality error angle, twenty-eight random samples were selected from a normal distribution with zero mean and unit standard deviation, since there were fourteen holes used to estimate orthogonality. Although there were thirteen physical holes, hole number 3 was repeated for horizontal fitting and vertical fitting. There were then two random numbers associated with each hole, one for $X$ and one for $Y$, designated by $\mathbf{R_x}$, $\mathbf{R_y}$. For each of the fourteen hole-centers the following simulated points were computed

$$x=\hat{x}+\hat{E}_x+R_x u_{co}(\hat{E}_x)$$
$$y=\hat{y}+\hat{E}_y+R_y u_{co}(\hat{E}_y) \tag{23}$$

The horizontal and vertical least squares lines through the appropriate new hole centers were computed using the normal equations for the horizontal lines and the appropriate equations for the vertical lines. The fitted horizontal and vertical lines took the form

$$\mathbf{y}=\beta_{\mathbf{0,h}}+\beta_{\mathbf{1,h}}\mathbf{x} \tag{24}$$

**Table 5 Orthogonality uncertainty (not expanded)**

| Mean Orthogonality (arc sec) | Sample Standard Deviation (arc sec) | Standard Uncertainty (arc sec) |
|---|---|---|
| −6.4 | 13.9 | 13.9 |

$$\mathbf{x}=\beta_{\mathbf{0,v}}+\beta_{\mathbf{1,v}}\mathbf{y}$$

Since the slopes were small and the tangent of a small angle is approximately the angle in radians we equated the slopes with angles. But in order to preserve the sign convention with respect to the horizontal axis the slope of the vertical line in Eq. (26) must have its sign changed. Thus the two angles were given by

$$\theta_1=\beta_{\mathbf{1,h}}$$
$$\theta_2=-\beta_{\mathbf{1,v}} \tag{25}$$

and the difference, or orthogonality error, was given by

$$\Delta\theta=\theta_2-\theta_1 \tag{26}$$

The uncertainty of the orthogonality was computed as

$$\mathbf{u^2_{co}}(\Delta\theta)=\mathbf{u^2_{co}}(\theta_2)+\mathbf{u^2_{co}}(\theta_1)=\mathbf{u^2_{co}}(\beta_{\mathbf{1,v}})+\mathbf{u^2_{co}}(\beta_{\mathbf{1,h}}) \tag{27}$$

For each horizontal and vertical line combination $\Delta\theta$ was computed using Eq. (24) through Eq. (26). This process was repeated a large number of times, $M$, and the estimated standard deviation $\hat{\sigma}$ was computed. The standard uncertainty was computed from

$$\mathbf{u^2_{co}}(\Delta\theta)=\hat{\sigma}^2\left(\mathbf{1}+\frac{\mathbf{1}}{\mathbf{M}}\right) \tag{28}$$

The results from a simulation with $M=1000$ are given in the Table 5.

## 4 Part Uncertainties by Coordinate Measuring Machine Measurements

The twenty-one parts, made according to Fig. 1, were measured on a CMM at NIST with an estimated uncertainty of 1 $\mu$m in positioning error. The following point locations were measured: the hole-center locations for the drilled holes, and the hole-centers of the milled holes. Five repeat measurements for each of these points were made on part numbers one through four, where a small variation between measurements was noted. Therefore, only two repeat measurements were performed on the remaining parts.

An analysis of variance procedure was used to isolate the manufacturing error from the coordinate measuring machine error. Manufacturing and measurement uncertainties were estimated. The analysis of variance procedure was applied to estimate the uncertainties of the locations of the hole-centers for both drilled and milled holes as well as to estimate the orthogonality. An estimate of the uncertainty of the distance between features was also developed.

**4.1 An Analysis of Variance Strategy.** For each machined part, the errors in hole-positions were measured by a CMM relative to a part coordinate system located at the lower left corner of

**Table 4 Line length uncertainties**

| | Length | | Uncertainty | | | |
|---|---|---|---|---|---|---|
| | Nominal (mm) | Estimated (mm) | Error (mm) | Variance ($\mu$m)$^2$ | Uncertainty ($\mu$m) | Expanded Uncertainty ($\mu$m) |
| 3–9 | 130 | 130 | 0.000 | 87.3 | 9.3 | 18.6 |
| 9–15 | 130 | 130 | 0.000 | 49.1 | 7.0 | 14.0 |
| 3–15 | 183.848 | 183.847 | 0.001 | 65.1 | 8.1 | 16.2 |

**Table 6 Uncertainty statistics for drilled-holes 3, 9, and 15. The uncertainties are not expanded uncertainties.**

| Summary Drilled Hole Statistics | | | | | | |
|---|---|---|---|---|---|---|
| | *X* Axis Location | | | | CMM Measurement | |
| Hole Number | Nominal (mm) | Error ($\mu$m) | Variance ($\mu$m)$^2$ | Uncertainty ($\mu$m) | Variance ($\mu$m)$^2$ | Uncertainty ($\mu$m) |
| 3 | 10 | 2.7 | 641 | 25.3 | 1.10 | 1.1 |
| 9 | 10 | 5.0 | 511 | 22.61 | 1.19 | 1.1 |
| 15 | 140 | −4.5 | 566 | 23.79 | 0.71 | 0.8 |
| | *Y* Axis Location | | | | CMM Measurement | |
| Hole Number | Nominal (mm) | Error ($\mu$m) | Variance ($\mu$m)$^2$ | Uncertainty ($\mu$m) | Variance ($\mu$m)$^2$ | Uncertainty ($\mu$m) |
| 3 | 10 | 8.0 | 1294 | 36.0 | 0.74 | 0.9 |
| 9 | 140 | −1.4 | 1209 | 34.8 | 0.68 | 0.8 |
| 15 | 140 | −1.6 | 1421 | 37.7 | 0.98 | 1.0 |

the inner 150 mm×150 mm square shown in Fig. 1. The *X* and *Y* locations of the centers of each drilled and milled hole on each of the twenty-one parts were measured a multiple number of times. Associated with each hole-center, two analysis of variance tables were formed, one for the *X*-measurements and one for the *Y*-measurements. Each table represented all of the location measurement errors for the same hole on each of the parts. The columns represented the repeated measurement errors from the nominal, as measured by the CMM. The measurement means were the calculated means for the repeated error measurements for the part numbers of the respective rows. The degrees of freedom were then listed in a column. Finally, the measurement uncertainties were the standard deviations of the repeated hole-location error measurements for that row. The measurement means had a grand mean and a variance (i.e., mean of means and a variance of means). These were taken as the manufacturing error and its variance for that hole. That is, these gave estimates of the manufacturing process uncertainties. An overall average variance could be computed from the column of measurement standard deviations, called the pooled variance, which was taken as an estimate of the uncertainty of the measurements. This uncertainty gave an estimate of the measurement process uncertainty. Once the manufacturing and measurement uncertainties had been estimated, the part uncertainties could be computed from the previous formulas.

The analysis of variance techniques were based on Dixon and Massey [29] and Mood and Graybill [30]. The notation used here is as follows: $n_i$, the number of measurements of the *i*-th part; $\mu_i$, the mean of the repeated measurements for part *i*; $s_i$, standard deviation of the repeated measurements for part *i*; $\mathbf{df}=\Sigma_{i=1}^{21}(\mathbf{n_i}-\mathbf{1})$, total degrees of freedom; $V_p(\mu)=(\Sigma_{i=1}^{21}(\mathbf{n_i})(\mu_i-\bar{\mu})^2)/(\mathbf{21}-\mathbf{1})$, estimate of the between part uncertainty; $V_p(s)=(\Sigma(\mathbf{n_i}-\mathbf{1})\mathbf{s_i^2})/\mathbf{df}$, estimate of the within part uncertainty. The *F*-ratio $\mathbf{F}=\mathbf{V_p}(\mu)/\mathbf{V_p}(\mathbf{s})$ was used to determine whether there is a significant difference between the two variance estimates (Montgomery and Peck [27]). For the cases of concern here, the test value for the *F* distribution at the 95% level with 20 degrees of freedom for $V_p(\mu)$ and 34 (i.e., 54–20) degrees of freedom for $V_p(s)$, since there are 54 total measurements for each hole center, over all of the parts, was approximately 1.89. The reader is referred to Dixon and Massey [29] for a discussion of the analysis of variance for a one-way fixed-effects classification model.

At this point we need to introduce some further terminology. Let

$$\mathbf{N}=\sum_{i=1}^{21}\mathbf{n_i} \tag{29}$$

be the total number of measurements over all the parts. Then, the pooled mean, called the mean manufacturing error or grand mean, is given by

$$\bar{\mu}=\frac{\Sigma_{i=1}^{21}\mathbf{n_i}\mu_i}{\mathbf{N}}. \tag{30}$$

The pooled standard deviation is

$$s_p=\sqrt{V_p(s)} \tag{31}$$

**Table 7 Uncertainty statistics for milled-holes 3, 9, and 15. The uncertainties are not expanded uncertainties.**

| Summary Milled Hole Statistics | | | | | | |
|---|---|---|---|---|---|---|
| | *X* Axis Location | | | | CMM Measurement | |
| Hole Number | Nominal (mm) | Error ($\mu$m) | Variance ($\mu$m)$^2$ | Uncertainty ($\mu$m) | Variance ($\mu$m)$^2$ | Uncertainty ($\mu$m) |
| 3 | 10 | 11.2 | 86.92 | 9.3 | 1.39 | 1.2 |
| 9 | 10 | 14.8 | 158.37 | 12.6 | 0.834 | 0.9 |
| 15 | 140 | 3.6 | 202.31 | 14.2 | 1.92 | 1.4 |
| | *Y* Axis Location | | | | CMM Measurement | |
| Hole Number | Nominal (mm) | Error ($\mu$m) | Variance ($\mu$m)$^2$ | Uncertainty ($\mu$m) | Variance ($\mu$m)$^2$ | Uncertainty ($\mu$m) |
| 3 | 10 | 11.2 | 73.15 | 8.6 | 0.30 | 0.6 |
| 9 | 140 | 9.6 | 246.05 | 15.7 | 0.19 | 0.4 |
| 15 | 140 | 4.7 | 237.28 | 15.4 | 0.33 | 0.6 |

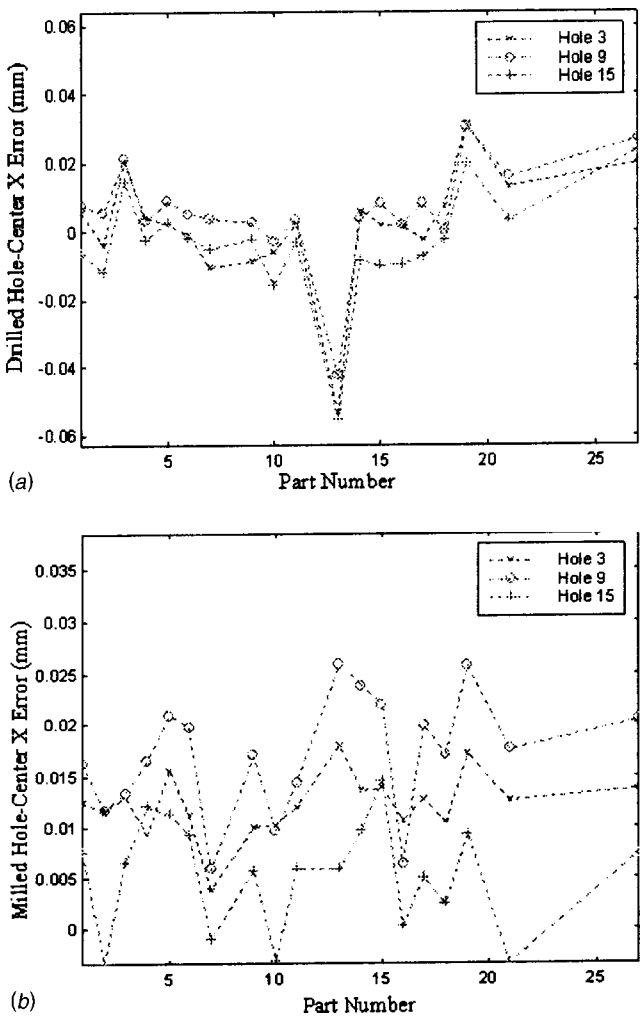


**Fig. 5 Mean *X* (a) errors for the centers of the drilled holes and mean *X* (b) errors for centers of milled holes. Vertical axis represents errors in mm. Horizontal axis represents part numbers.**

An estimate of the standard uncertainty of the grand mean is given by

$$\mathbf{u}=\frac{\mathbf{s_p}}{\sqrt{\mathbf{N}}} \tag{32}$$

An estimate of the uncertainty of a future measurement sample is given by

$$\mathbf{u_f}=\left(\sqrt{\mathbf{1}+\frac{\mathbf{1}}{\mathbf{N}}}\right)\mathbf{s_p} \tag{33}$$

The corresponding expanded uncertainty of a future measurement can then be taken as

$$\mathbf{U_f}=\mathbf{2u_f} \tag{34}$$

**4.2 Hole-Center Location Uncertainties for the Manufactured Parts.** Tables 6 and 7 show the *X* and *Y* errors of the hole centers 3, 9, 15, the center location uncertainties, and the measurement uncertainties. The measurement uncertainties are approximately the quoted uncertainty for the CMM at NIST. As the tables show the drilled hole uncertainties are higher than the milled hole uncertainties. These are typical for the other holes in Fig. 1. Typical error measurements are shown in Fig. 5.

Figure 5(*a*) shows the *X* mean measured errors for the centers of the three drilled holes numbered 3, 9 and 15 in Fig. 5. *Y* mean measured errors show similar error formations. The first thing to be noted about the measurements is that part 13 shows a significant negative *X*-mean error for all three drilled holes compared to the other parts. This appears to be reflected in the *Y*-mean errors for that part also. Notice also the significant center location errors for parts 3, 19, 21 and 27 (a mistaken part blank number for part 20). Figure 5(*b*) shows sharp error differences for the *X* measurements of milled holes 3, 9 and 15 which are also reflected in the *Y* measurements. Note that the error range for the milled hole errors is less than that of the drilled hole center errors.

Figure 6 shows the position errors of the holes for the predicted, milled and drilled peripheral hole-centers.

The arrows show the direction of the hole center error and the magnitude of the arrows represent scaled magnitudes of the errors. Note that the model predicted directions and magnitudes (Fig. 6(*a*)) closely align with those for the milled holes (Fig. 6(*b*)), whereas the magnitudes and directions of the drilled hole centers (Fig. 6(*c*)) vary drastically from the predicted and milled hole centers.

**4.3 Estimating the Uncertainty of a Machined Length Feature From CMM Measurements.** The lengths and uncertainties of these lengths were computed for the measured distances between holes 3, 9 and 15 on the machined parts. The summary statistics of the measured errors and uncertainties are given for the three hole-center features in Tables 8 and 9. The error variance estimates given in these tables were computed as the pooled variance of the mean. The uncertainty estimates were computed as the square roots of the respective variance estimates. Table 8 gives the results for the drilled hole-centers for feature holes 3, 9, and 15, while Table 9 gives the results for the milled square hole-centers for the same feature holes. The tables give the nominal coordinates of the hole-centers, relative to the part origin in the lower left corner. Although not shown in the tables, the measurement uncertainties fell approximately at the quoted CMM value of 1 $\mu$m.

Table 10 gives the summary results of the center-to-center length errors for drilled and milled hole-centers as well as the predicted length errors. The table also includes the expanded uncertainties of the length errors.

**4.4 Estimating the Uncertainty of Machined Part Hole Center Orthogonality From CMM Measurements.** The peripheral milled hole centers were selected as points to be used for estimating orthogonality. The milled holes were designed to have their nominal centers form lines parallel to the edges of the parts. Two nominally orthogonal lines of holes (the bottom row and left side row) were selected to estimate the uncertainties in the orthogonality of these two lines of holes. The procedure of estimating orthogonality was as follows.

For the centers of the holes along the *X*-axis a least squares fit of the line form $y=m_h x+b$ was made for each of the repetition error measurements for each of the parts. This produced a table of estimated slope values for $m_h$. Since the deviation of $m_h$ from zero was small the values of $m_h$ could be used as angle estimates since for small angles $\tan(a)\approx a$ in radians and $m_h$ is the tangent of the slope angle. Next the leftmost vertical line of hole centers was fit with an equation of the form $x=m_v y+b$. The sign of the resulting slope had to be reversed and then it could be added to the horizontal slope to determine the orthogonality error. This calculation is similar to that leading to Eq. (25) and Eq. (26). The results are summarized in Table 11. Note that the variance of the metrology uncertainties is an order of magnitude less than the variance of the manufacturing error so that the measured and manufacturing variances could be considered approximately equal as expected.

## 5 Discussion

When we compared the predicted errors computed from LBB measurements for the peripheral holes, the mean errors of the

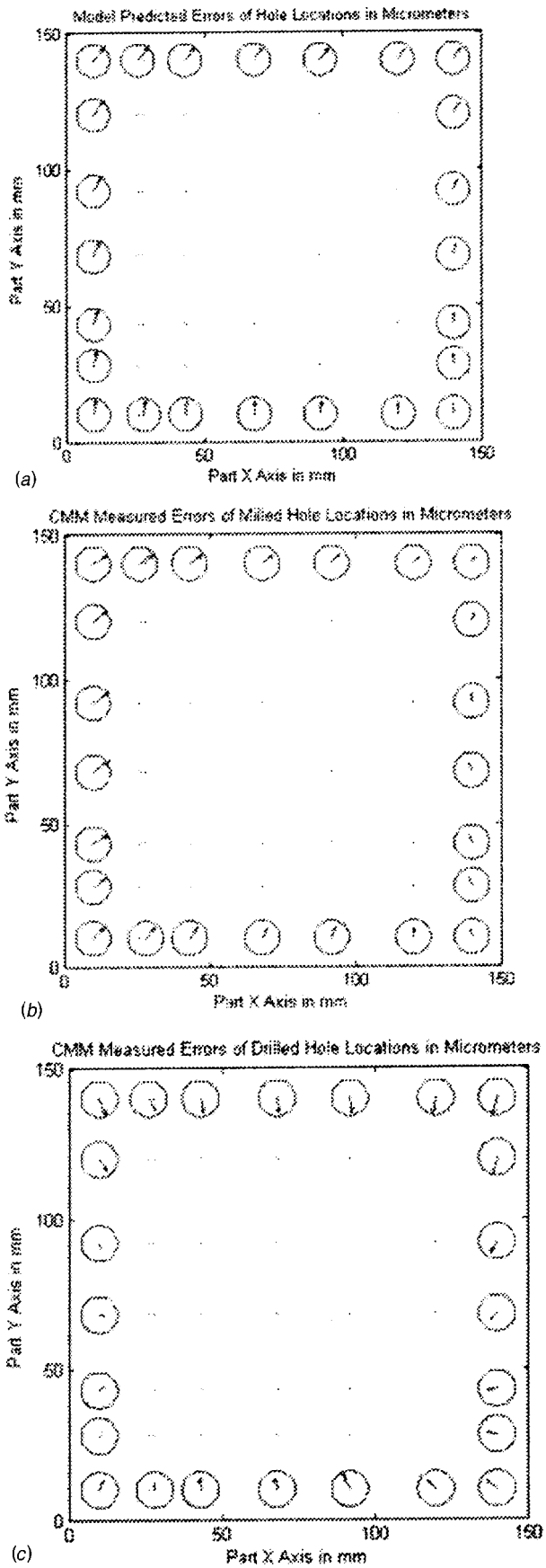


**Fig. 6 Arrows represent the direction and scaled locations of the predicted (*a*), the milled (*b*), and the drilled (*c*) hole center locations**

**Table 8 Manufactured length uncertainties between drilled-hole centers. The uncertainties are not expanded uncertainties.**

| Manufactured Length Between Drilled Holes | | | | | |
|---|---|---|---|---|---|
| Hole-Hole | Nominal Length (mm) | Actual Length (mm) | Actual Error ($\mu$m) | Actual Variance ($\mu$m)$^2$ | Actual Uncertainty ($\mu$m) |
| 3 to 9 | 130 | 129.978 | 21.6 | 2549 | 50.5 |
| 9 to 15 | 130 | 129.991 | 9.5 | 1097 | 33.1 |
| 3 to 15 | 183.84776 | 183.843 | 22.5 | 1997 | 44.7 |

measured parts tended to be larger. The manufacturing uncertainties for a given feature measurement were greater than those predicted by the LBB measurements. The signs of the errors for both the predicted errors and the measured errors tended to be consistent for the milled holes but not for the drilled holes as shown in Fig. 6. Tables 6 and 7 indicate that the uncertainties associated with drilling operations tend to be larger than those for milling operations. A possible explanation for this may be the fact that a drill bit has a tendency to hop slightly before the flutes bite into the material being machined. The predicted LBB uncertainties fall less than both the drilled and milled center-to-center uncertainties but tend to be closer to the milled uncertainties. This is reasonable considering the results shown in Fig. 6.

The range of the predicted hole center variances of the *X*-errors, based upon the LBB measurements, fell between 10.6 $\mu$m$^2$ and 24.6 $\mu$m$^2$. For the *Y*-errors, the predicted variances fell between 43.7 $\mu$m$^2$ and 52.4 $\mu$m$^2$. For the parts measured by the CMM the variances were significantly larger. The *X*-machine error variances for the drilled holes fell between 511 $\mu$m$^2$ and 641 $\mu$m$^2$. For the milled holes the center *X*-machine errors ranged from 86.9 $\mu$m$^2$ to 202.3 $\mu$m$^2$. The *Y*-machine error variances tended to be larger for both drilled and milled hole center errors. For the drilled holes the *Y*-machine error variances fell between 1209 $\mu$m$^2$ and 1421 $\mu$m$^2$. For the milled holes the *Y*-machine error variances fell between 73.2 $\mu$m$^2$ and 246.1 $\mu$m$^2$. We noted that the *Y*-machine error variances were in general greater than the *X*-machine error variances in both the model prediction and CMM measurement cases. As a diagnostic tool this suggests a potential malfunction in the *y*-axis of the machining center.

The differences between the uncertainties for the drilling and milling of hole centers are carried over to the estimates of hole-to-hole center lengths. These are shown in Tables 8 and 9. The variances for the center-to-center lengths for the drilled holes ranged from 1097 $\mu$m$^2$ to 2549 $\mu$m$^2$, whereas for the milled holes they ranged from 305 $\mu$m$^2$ to 367 $\mu$m$^2$. The work of Wilhelm, Srinivasan and Farabaugh [5] showed that the position errors of the test part holes fall in general within two standard deviations of the measured machine errors. Their work however was conducted under controlled laboratory conditions. The parts in this study were not milled under controlled conditions, but under ordinary shop environment conditions. The results of this study suggest that for the particular machining center used, the potential length errors of manufactured parts could fall as far away as seven standard deviations of the measured machine errors for drilled holes

**Table 9 Manufactured length uncertainties between milled hole centers. The uncertainties are not expanded uncertainties.**

| Manufactured Length Between Milled Hole Centers | | | | | |
|---|---|---|---|---|---|
| Hole-Hole | Nominal Length (mm) | Actual Length (mm) | Actual Error ($\mu$m) | Actual Variance ($\mu$m)$^2$ | Actual Uncertainty ($\mu$m) |
| 3 to 9 | 130 | 129.998 | 1.6 | 325 | 18 |
| 9 to 15 | 130 | 129.989 | 11.2 | 367 | 19.2 |
| 3 to 15 | 183.84776 | 183.838 | 10.0 | 305 | 17.5 |

**Table 10 A comparison of the upper and lower expanded uncertainty limits for the hole-to-hole lengths based on the CMM measurements and the model estimates based on the LBB machine measurements**

| Drilled Hole Expanded Uncertainty Range | | | | |
|---|---|---|---|---|
| Center-to-Center Lines | Lower Uncertainty Bound ($\mu$m) | Mean Length Error ($\mu$m) | Upper Uncertainty Bound ($\mu$m) | Range Width ($\mu$m) |
| 3 to 9 | −122.6 | 21.63 | 122.6 | 245.3 |
| 9 to 15 | −75.7 | 9.51 | 75.7 | 151.4 |
| 3 to 15 | −111.9 | 22.45 | 111.9 | 223.8 |
| Milled Hole Expanded Uncertainty Range | | | | |
| Center-to-Center Lines | Lower Uncertainty Bound ($\mu$m) | Mean Length Error ($\mu$m) | Upper Uncertainty Bound ($\mu$m) | Range Width ($\mu$m) |
| 3 to 9 | −37.6 | 1.59 | 37.6 | 75.2 |
| 9 to 15 | −49.6 | 11.17 | 49.6 | 99.2 |
| 3 to 15 | −45.0 | 9.96 | 45.0 | 90.0 |
| Expanded Uncertainty Estimates Based on LBB Machine Metrology | | | | |
| Center-to-Center Lines | Lower Uncertainty Bound ($\mu$m) | Mean Length Error ($\mu$m) | Upper Uncertainty Bound ($\mu$m) | Range Width ($\mu$m) |
| 3 to 9 | −18.7 | 0.00 | 18.7 | 37.4 |
| 9 to 15 | −18.2 | 4.2 | 18.2 | 36.4 |
| 3 to 15 | −16.5 | 0.3 | 16.5 | 33.0 |

and three for milled holes. This indicates that machining uncertainties under a production environment can potentially be much larger than those obtained under controlled conditions. The expanded center-to-center uncertainty ranges shown in Table 10 are consistent with the previous findings. The ratios of the drilled hole ranges to the predicted ranges fell between four and seven, whereas the ratios for the milled holes fell between two and three.

The predicted mean orthogonality error from Table 5 is −6.4 arc sec and the uncertainty is 13.9 arc sec. These were based on the Monte Carlo method of estimating orthogonality from the machine tool model and LBB measurements. From Table 11 the mean manufacturing orthogonality error from the CMM measurements was −1.5 arc sec with an uncertainty of 28.7 arc sec for drilled holes. For milled holes the mean orthogonality error was 0.4 arc sec with an uncertainty of 15.5 arc sec. In this case the model estimates over-predict the orthogonality error. However the model results produce an uncertainty near to that for the milled-hole orthogonality. The ratio of the drilled-hole orthogonality uncertainty to the metrology uncertainty was 7.9. In the case of the milled-hole orthogonalities the ratio was 4.8.

In all of the analysis of variance tables the $F$ tests indicated that there was a great deal of variability between parts.

Since this was a limited study a relation between the predicted uncertainties and the measured uncertainties in a production environment could not be quantified. However, the authors feel that this could be a significant result, if established, and encourage further research along this line. But what does seem clear is that uncertainties are process dependent.

**Table 11 Summary of the orthogonality statistics from CMM measurements**

| Summary Drilled Hole Orthogonality Statistics | | | | |
|---|---|---|---|---|
| Manufacturing Error (arc sec) | Manufacturing Variance (arc sec)$^2$ | Manufacturing Uncertainty (arc sec) | Metrology Variance (arc sec)$^2$ | Metrology Uncertainty (arc sec) |
| −1.470 | 825 | 28.7 | 12.08 | 3.6 |
| Summary Milled Hole Orthogonality Statistics | | | | |
| Manufacturing Error (arc sec) | Manufacturing Variance (arc sec)$^2$ | Manufacturing Uncertainty (arc sec) | Metrology Variance (arc sec)$^2$ | Metrology Uncertainty (arc sec) |
| 0.364 | 239 | 15.5 | 10.00 | 3.2 |

## 6 Conclusions

There are a number of conclusions that can be drawn from this study. The first and foremost is that machining uncertainties can be estimated for production machines but uncertainties obtained from measurements of machine error components account for only a small part of machined part uncertainties. These uncertainties, of course, only apply to the individual machine being studied, however it would be interesting to do a parallel study on a production machine from the same family to determine whether there are any commonalities. It also seems clear that further study is needed to determine those aspects of the machining processes that lead to the significant uncertainties affecting machined parts.

In terms of machine metrology, setting up the particular LBB for measuring the machine tool component errors was cumbersome, but it did provide measurements for all of the components necessary to model the machine tool. It was possible to take all of the measurements in a reasonably short time without changing fixtures for each component measurement.

The law of Propagation of Uncertainties provided a means of estimating both point location and length uncertainties when combined with an adequate kinematic model of the machine tool under study. There were uncertainties, such as for orthogonality, where the law was not applicable directly. These uncertainties occurred in cases where there were no clearly understood functional relationships between quantities that would allow the law to be applied. In these cases some form of simulation or Monte Carlo technique would have to be applied to estimate the uncertainties.

Finally, it was clear that there should be further studies to try and estimate and separate out the nonstationary effect of the thermal drift in order to obtain a proper estimate of the machine tool error component variability. These studies should also investigate possible measurement techniques to determine the cross-correlation of the various machine tool error components.

## Acknowledgments

The authors wish to thank the many members of the NIST staff who participated in various ways to make this project a success.

Bruce R. Borchardt performed measurements of the manufactured parts on a CMM. Robert R. Clary, a machinist, was instrumental in running the vertical machining center during the measurement of the machine with the laser ball bar but also during the machining of the parts. M. Alkan Donmez supervised the overall case study and provided invaluable consulting on machine tool metrology. Richard Rhorer played an important part in the early design of the experiment and part design. Johannes A. Soons designed the final part selected, provided machine tool programming and metrology consultation. We also thank Stephan Leigh of the NIST Statistical Engineering Division for his many helpful suggestions. Thanks are also due to the journal referees for their insightful comments.

## References

[1] International Organization for Standardization, Guide to the Expression of Uncertainty in Measurement.
[2] Taylor, B. N., and Kuyatt, C. E., 1994, ''Guidelines for Evaluating and Expressing the Uncertainty of NIST Measurement Results,'' NIST Technical Note 1297, National Institute of Standards and Technology, Gaithersburg, MD, 20899.
[3] American National Standards Institute, 1997, ''American National Standard for Expressing Uncertainty—U.S. Guide to the Expression of Uncertainty in Measurement,'' ANSI/NCSL Z540-2-1997.
[4] Gilsinn, D. E., and Ling, A. V., 2002, ''Comparative Statistical Analysis of Test Parts Manufactured in Production Environments,'' NISTIR 6868, National Institute of Standards and Technology, Gaithersburg, MD, 20899-8910.
[5] Wilhelm, R. G., Srinivasan, N., and Farabaugh, F., 1997, ''Part Form Errors Predicted From Machine Tool Performance Measurements,'' CIRP Ann., **46**, pp. 471–474.
[6] Chatterjee, S., 1997, ''An Assessment of Quasi-Static and Operational Errors in NC Machine Tools,'' J. Manuf. Syst., **16**(1), pp. 59–68.
[7] Shin, Y. C., and Wei, Y., 1992, ''A Statistical Analysis of Positional Errors of a Multiaxis Machine Tool,'' Precis. Eng., **14**, pp. 139–146.
[8] Kaminski, J., and Crafoord, R., 1991, ''Position Accuracy of Drilled Holes,'' CIRP Ann., **40**, pp. 503–506.
[9] Lehtihet, E. A., and Gunasena, U. N., 1990, ''Statistical Models for the Relationship Between Production Errors and the Position Tolerance of a Hole,'' CIRP Ann., **39**, pp. 569–572.
[10] Lee, S. J., Eman, K. F., and Wu, S. M., 1987, ''An Analysis of the Drill Wandering Motion,'' ASME J. Eng. Ind., **109**, pp. 297–305.
[11] Fujii, H., Marui, E., and Ema, S., 1986, ''Whirling Vibration in Drilling, Part 1: Cause of Vibration and Role of Chisel Edge,'' ASME J. Eng. Ind., **108**, pp. 157–162.
[12] Fujii, H., Marui, E., and Ema, S., 1986, ''Whirling Vibration in Drilling, Part 2: Influence of Drill Geometries, Particularly of the Drill Flank, on the Initiation of Vibration,'' ASME J. Eng. Ind., **108**, pp. 163–168.
[13] Fujii, H., Marui, E., and Ema, S., 1988, ''Whirling Vibration in Drilling, Part 3: Vibration Analysis in Drilling Workpiece With a Pilot Hole,'' ASME J. Eng. Ind., **110**, pp. 315–321.
[14] Magrab, E. B., and Gilsinn, D. E., 1984, ''Buckling Loads and Natural Frequencies of Drill Bits and Fluted Cutters,'' ASME J. Eng. Ind., **106**, pp. 196–204.
[15] Shen, Y., and Duffie, N. A., 1995, ''An Uncertainty Analysis Method for Coordinate Referencing in Manufacturing Systems,'' ASME J. Eng. Ind., **117**, pp. 42–48.
[16] Shen, Y., and Duffie, N. A., 1991, ''Uncertainties in the Acquisition and Utilization of Coordinate Frames in Manufacturing Systems,'' CIRP Ann., **40**(1), pp. 527–530.
[17] Bauer, W. F., 1958, ''The Monte Carlo Method,'' J. Soc. Ind. Appl. Math., **6**(4), pp. 438–451.
[18] Yau, H., 1997, ''Evaluation and Uncertainty Analysis of Vectorial Tolerances,'' Precis. Eng., **20**, pp. 123–137.
[19] Phillips, S. D., Borchardt, B., Estler, W. T., and Buttress, J., 1998, ''The Estimation of Measurement Uncertainty of Small Circular Features Measured by Coordinate Measuring Machines,'' Precis. Eng., **22**, pp. 87–97.
[20] ASME B5.54-1992, 1993, *Methods for Performance Evaluation of Computer Numerically Controlled Machining Centers*, The American Society of Mechanical Engineers, New York.
[21] Ziegert, J. C., and Mize, C. D., 1994, ''The Laser Ball Bar: A New Instrument for Machine Tool Metrology,'' Precis. Eng., **16**, pp. 259–267.
[22] Srinivasa, N., and Ziegert, J. C., 1996, ''Automated Measurement and Compensation of Thermally Induced Error Maps in Machine Tools,'' Precis. Eng., **19**, pp. 112–132.
[23] Schmitz, T., and Ziegert, J., 1998, ''Premachining Computer Numerical Control Contour Validation,'' Precis. Eng., **22**, pp. 10–18.
[24] Donmez, M. A., 1985, ''A General Methodology for Machine Tool Accuracy Enhancement: Theory, Application and Implementation,'' Ph.D. Thesis, Purdue University.
[25] Coleman, H. W., and Steele, W. G., 1999, *Experimentation and Uncertainty Analysis for Engineers*, John Wiley & Sons, Inc., New York.
[26] Wheeler, A. J., and Ganji, A. R., 1996, *Introduction to Engineering Experimentation*, Prentice Hall, Englewood Cliffs.
[27] Montgomery, D. C., and Peck, E. A., 1992, *Introduction to Linear Regression Analysis*, John Wiley & Sons, Inc., New York.
[28] Mandel, J., 1984, ''Fitting Straight Lines When Both Variables are Subject to Error,'' J. Quality Technol., **16**, pp. 1–14.
[29] Dixon, W. J., and Massey, Jr., F. J., 1957, *Introduction to Statistical Analysis*, McGraw-Hill Book Company, Inc., New York.
[30] Mood, A. M., and Graybill, F. A., 1963, *Introduction to the Theory of Statistics*, McGraw-Hill Book Company, Inc., New York.